

Feature Article

Role of Dislocations in Silver Halide Photography

J. W. Mitchell

Department of Physics, University of Virginia, Charlottesville, Virginia 22901

Dislocations and donor centers have important functions in the optimization of the performance of silver halide emulsion grains. The basic properties of dislocations relevant to photographic sensitivity together with the experimental observations which established these properties are reviewed in this paper. Internal latent image and internal particles of photolytic silver are formed during exposure of AgCl and AgBr crystals, sensitized with Ag₂O and Ag₂ donor centers, by the separation of Ag atoms along the dislocation lines. The surface sites of termination of dislocations have enhanced reactivity compared with low-energy surfaces. Dissolution, chemical sensitization, and the initiation of surface chemical development occur at higher rates at these sites. These properties led to the concept of the dislocation sensitivity center. Development centers are formed by the combination of Ag atoms with Ag₂ latent image growth nucleus precursors at the surfaces of dislocation sensitivity centers. The formation of Ag₂ molecules along the sub-surface dislocation of the center has to be minimized. Microcrystals of AgCl and AgBr with dislocations introduced during nucleation and initial growth pass into solution at a high rate during a short period of ripening leaving dislocation-free growth nuclei. For stable distributions of dislocations in microcrystals, concentration gradients of halide ions have to be established in heterogeneous crystals. Controlled densities of dislocations are introduced to reduce the elastic strains associated with steep concentration gradients. In double-structure grains with a higher iodide shell and in triple-structure grains with a higher iodide narrow zone, the concentration gradients can be established by the addition of a fine dispersion of Ag(Br,I) particles or of an iodide ion releasing compound. The resulting dislocation distributions are stable because of the immobility of the iodide ions in the crystal. The mechanisms involved in the creation of dislocations in structured tabular microcrystals are discussed.

Journal of Imaging Science and Technology 41: 1–12 (1997)

Introduction

The full appreciation of the significance and the effective utilization of the concepts of dislocations and donor centers is essential for the design of the grains of high-speed negative and direct positive silver halide emulsions of the highest achievable performance. Sensitivity is determined by the distribution and density of dislocations and donor centers, and microcrystals of high purity and perfection with neither dislocations nor donor centers have a very low sensitivity.

The roles of donor centers and of Ag₂ latent image growth nucleus precursors in the photoaggregation theory of la-

tent image formation were discussed in a recent paper¹ without particular reference to the role of dislocations in the chemical and photochemical processes.^{2–4} In this paper, the basic properties of dislocations are summarized and the experimental work which first established many of these properties is presented.⁵ It is significant for photographic technology that this experimental work was carried out with thin sheet crystals of AgCl and AgBr, sensitized with Ag₂O and Ag₂ molecules, in which the dislocations were decorated during exposure by the almost continuous separation of particles of photolytic silver. The reasons for the enhanced reactivity of the surface sites of termination of dislocations are discussed. This work led to the introduction of the important concept of the dislocation sensitivity center.⁶

Dislocations are high-energy lattice defects which are eliminated from growth nuclei for pure AgBr microcrystals by a short period of ripening after nucleation.⁷ Stable distributions of dislocations are created in these crystals to partially relax the lattice strains associated with steep concentration gradients of iodide ions.^{8,9} The role of both dislocations and donor centers in determining the sensitivity of emulsions of the core/shell type is emphasized.

Dislocations in Crystals

When single crystals of high perfection are subjected to shear stresses, plastic deformation begins at the surface with the formation of a linear surface terrace associated with an area of partial slip on a closely packed glide plane (Fig. 1). The boundary of the slipped area is a linear crystal

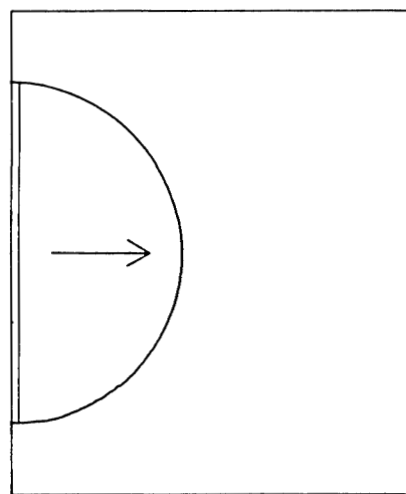


Figure 1. Surface terrace of unit width and dislocation half-loop formed by partial slip on a glide plane. The dislocation is in the edge orientation when the glide vector is at right angles and in the screw orientation when it is parallel to the line.

Original manuscript received July 29, 1996.

IS&T Honorary Member

© 1997, IS&T—The Society for Imaging Science and Technology

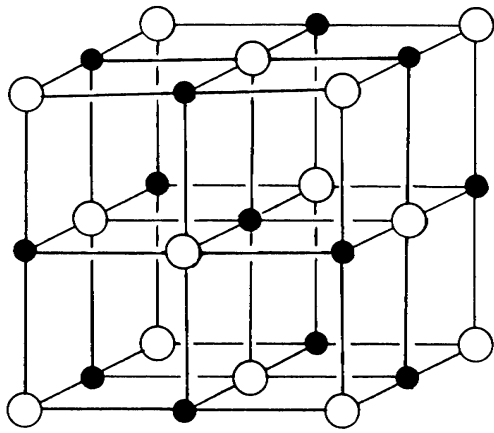


Figure 2. The unit cell for AgCl and AgBr crystals showing $\{111\}$, $\{110\}$, and $\{001\}$ glide planes and the 12 $\langle 110 \rangle$ face diagonal glide directions.

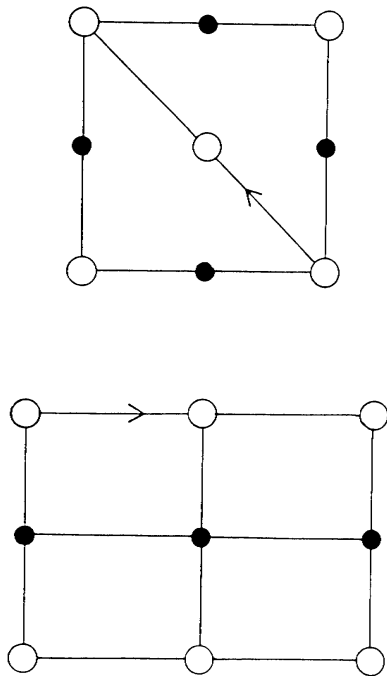


Figure 3. The $\{001\}$ and $\{110\}$ glide planes with the $\langle \bar{1}10 \rangle$ unit glide vector. The magnitude of the unit vector $b = 1/2 a \langle \bar{1}10 \rangle = a/\sqrt{2} / 2$.

lattice imperfection or a dislocation half-loop. The slip process is characterized by a slip direction or a slip vector parallel to a row of closely packed atoms or a row of like ions on the glide plane. Within the half-loop there is a relative displacement of the crystal on the two sides of the glide plane by one crystal lattice vector. We will see later that the formation of these half-loops at the surface by plastic deformation before exposure is responsible for kink desensitization. The slip vector is constant around the loop but its orientation changes with respect to the dislocation line. The dislocation line is in the edge orientation when the vector is at right angles and in the screw orientation when it is parallel to the line.

In AgCl and AgBr crystals, slip occurs in $\langle 110 \rangle$ directions parallel to the face diagonals of the unit cell (Fig. 2).

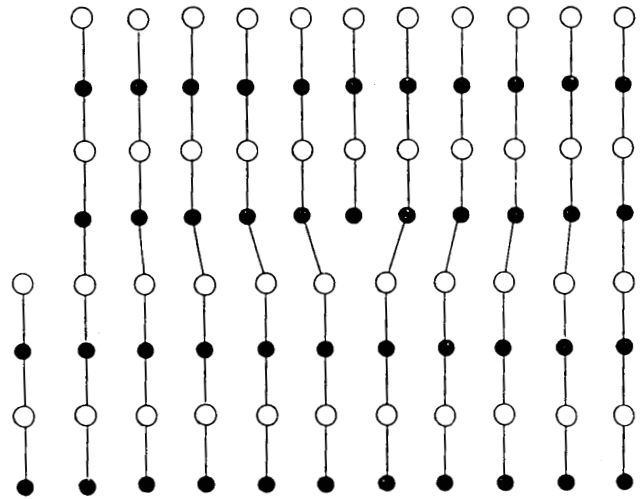


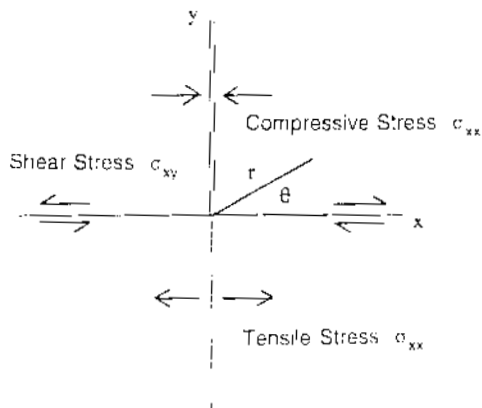
Figure 4. Edge dislocation with associated surface terrace on an atomic scale. This shows the structure of a $(11\bar{2})$ plane of a silver halide crystal with an edge dislocation and associated surface terrace generated by glide on a $\{111\}$ plane in a $[\bar{1}10]$ direction.

These are along rows of X^- and parallel rows of Ag^+ ions (see footnote on p. 194 of Ref. 1). In these crystals, slip can occur on any plane containing a $\langle 110 \rangle$ direction, for example, $\{001\}$, $\{110\}$, or $\{111\}$ planes. This pencil glide allows a circular prismatic edge dislocation loop to be formed with a $\langle 110 \rangle$ slip vector. The magnitude of the lattice slip vector is equal to the interatomic distance along a row, $b = 1/2 a \langle 110 \rangle$ (Fig. 3).

On an atomic scale, the creation of the edge segment of the dislocation half-loop on a $\{111\}$ plane by partial slip in a $\langle \bar{1}10 \rangle$ direction is illustrated in Fig. 4. We have a $(11\bar{2})$ plane of ions at right angles to the trace of the $\{111\}$ glide plane. The rows of ions are parallel to the $\langle \bar{1}10 \rangle$ direction. The edge dislocation results from the displacement of two half-planes of ions into the crystal with the production of a surface terrace of unit width. These half-planes terminate at the glide plane. Their propagation across the glide plane produces a relative translation by one lattice slip vector, $b = 1/2 a [\bar{1}10]$ without the introduction of observable lattice imperfection on the glide plane. The Burgers vector of the dislocation line is defined by taking a closed right-handed circuit around the positive $[11\bar{2}]$ direction of the line from ion to ion in this diagram. The same circuit is then stepped around the corresponding ions in a perfect crystal. The closure failure gives the Burgers vector of the dislocation which is, in this example, $\mathbf{b} = 1/2 a [\bar{1}10]$ ^{10,11}

A dislocation is associated with an internal stress field that falls off as $1/r$ from the dislocation line and produces a local increase in the elastic strain energy density (Fig. 5). The stress field of an edge dislocation has maximum compressive and tensile stresses and zero shear stress in a plane through the edge at right angles to the glide plane. It has maximum shear stress and zero compressive stress at the glide plane. The screw dislocation has a pure shear stress field. The superposition of an applied shear stress may cause displacement of a dislocation across a glide plane. This produces a relative translation by one lattice slip vector. These properties of dislocations are discussed in the books of Friedel,¹² Nabarro,¹³ and Hirth and Lothe.¹⁴

Properties of dislocations in the edge orientation are particularly important for photographic sensitivity. In deliberately established favorable conditions, dislocations are involved in the localization of surface chemical sensitization, localized formation of surface and internal



$$\begin{aligned}\sigma_{xx} = \sigma_{11} &= -(D/r) \sin \theta (2 + \cos 2\theta) \\ \sigma_{yy} = \sigma_{22} &= (D/r) \sin \theta \cos 2\theta \\ \sigma_{zz} = \sigma_{33} = \nu (\sigma_{11} + \sigma_{22}) &= -(2\nu D/r) \sin \theta \\ \sigma_{xy} = \sigma_{12} = \sigma_{21} &= (D/r) \cos \theta \cos 2\theta \\ \sigma_{xz} = \sigma_{yz} = \sigma_{13} = \sigma_{23} &= 0 \\ D &= Gb/2\pi(1 - \nu)\end{aligned}$$

Figure 5. The internal stress field of an edge dislocation showing compressive and tensile stresses on the $x = 0$ plane and shear stresses on the $y = 0$ plane. The maximum stresses are for $r = b$, the magnitude of the unit slip vector. G is the shear modulus and ν , Poisson's ratio.

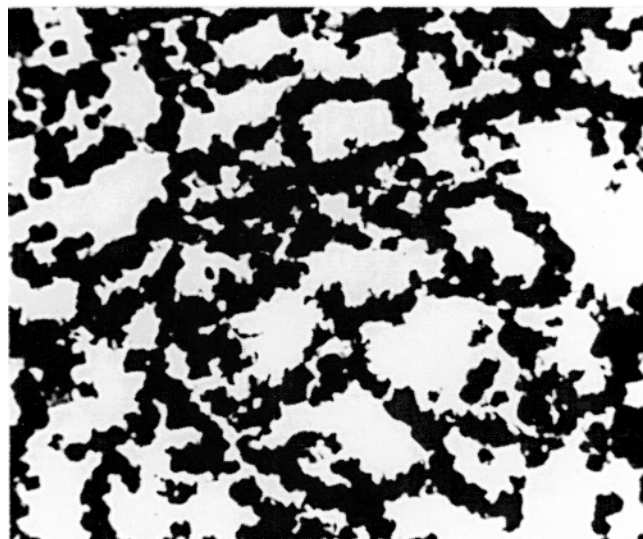


Figure 6. Development centers along lines of intersection of a substructure with an internal plane of an exposed AgBr crystal (X 950).⁶

latent image centers, initiation of surface chemical development, and formation of internal print-out silver.

Direct Observations and Properties of Dislocations within Crystals

The basic theoretical concepts presented above were appreciated before the summer of 1952 (Ref. 15), but there had been no direct observations of dislocations as internal linear lattice imperfections. The first observations of actual dislocations within crystals were made in November 1952 during the course of research on the nature and distribution of the internal latent image with AgBr crystals sensitized with Ag_2O and Ag_2 donor centers.^{16,17} Thin

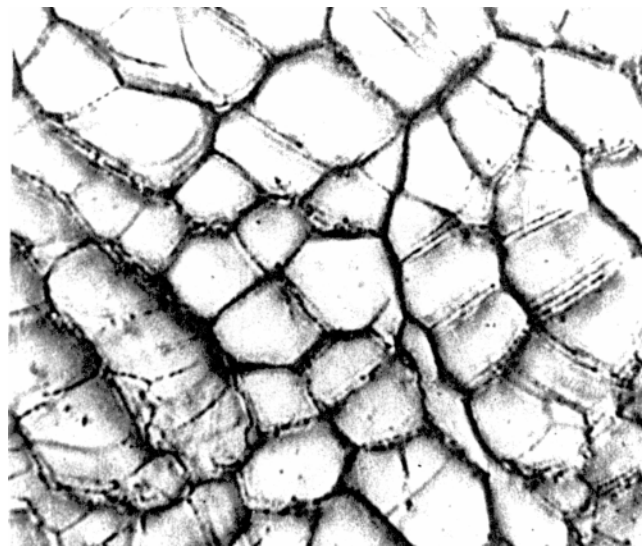


Figure 7. Polyhedral substructure of an AgBr crystal revealed by the separation of Ag atoms along dislocation arrays of subboundaries during exposure in long-wave tail of absorption band (X 1,050).⁶



Figure 8. Subboundaries of mosaic structure with hexagonal networks of dislocations (X 1,000).

sheet crystals, exposed and then developed with a surface developer, gave no image. When the surface was treated with a solvent, followed by the surface developer, development specks were produced which appeared to outline the boundaries of a substructure (Fig. 6). Another section of the same crystal was then given a longer exposure. The boundaries of the substructure were revealed in three dimensions for the first time (Fig. 7). Exposure resulted in the almost continuous separation of particles of silver along the dislocation segments of the substructure making them visible with good contrast by high-resolution optical microscopy. Substructure interfacial boundaries with hexagonal networks of dislocations and larger angle sub-grain boundaries are shown in Fig. 8. The internal development centers of Fig. 6 were produced along the dislocation segments by a shorter exposure. With the visible violet radiation used, the dislocations were decorated to a depth of about 30 μm below the surface.

The Ag atoms and Ag_n^+ clusters, formed by the combination of Ag_0^+ ions and electrons, separate in the tensile regions of dislocations in the edge orientation, lowering the free energy. Jogs and edge segments along

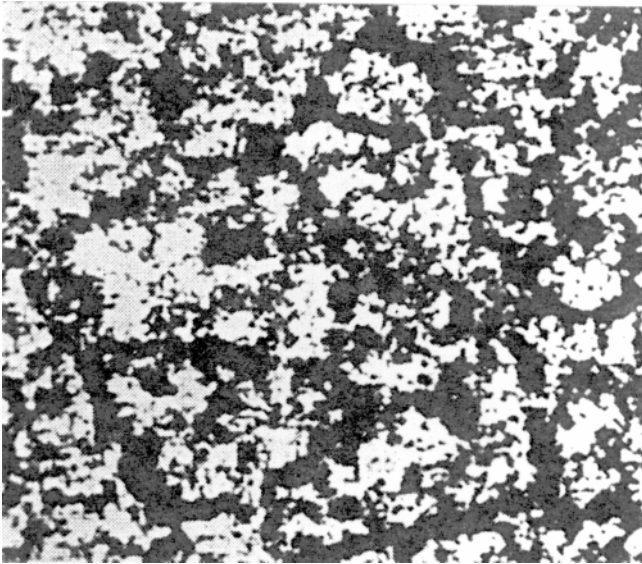


Figure 9. Development on an internal plane intersecting the boundaries of a polyhedral substructure at centers produced by the diffusion of Ag atoms from the outer surface (X 1,060).²

screw dislocations allow similar decoration during exposure. These properties were clearly demonstrated by the vacuum deposition of Ag atoms from an atomic beam on the surface of an AgBr crystal. For the first time in 1955 Ag atoms were shown to dissociate into electrons and Ag^+ ions which diffuse into the crystal to combine and produce development centers along the dislocation segments (Fig. 9) (Ref. 18a,b). Gold atoms did not diffuse in this way.

The remarkable involvement of dislocations in the mosaic structure of a real crystal was also demonstrated at this time. The essential features of this structure were envisaged by Darwin in 1914 in his theoretical work on the intensity and angular width of x-ray reflections from crystals.^{19,20} He calculated the intensity of the reflection of an x-ray beam by an ideally perfect crystal and found a value 1/20th to 1/30th of the observed value. The angular width of the reflection was about 5" of arc compared with the observed values of minutes of arc. Darwin concluded that real crystals were imperfect and repeated the calculations for a model with an ideally imperfect crystal.²¹ In this model, the crystal was supposed to be a conglomerate of small blocks of perfect crystal with adjacent blocks not accurately fitted together. The blocks were approximately parallel to each other with orientations distributed through an angular range of many minutes of arc around any mean direction. The values of the intensity and angular width of the reflections calculated with this model were close to the observed values. The term *mosaic* for this structure of small blocks appears to have been introduced at a conference organized by Ewald in 1925.^{22,23} This model was still accepted in 1952.

The nature of the actual mosaic structure of a crystal was first observed in 1953 with sensitized lightly annealed thin sheet crystals of AgBr (Fig. 10). Exposure of the crystals caused the formation of particles of silver over planar boundaries between polyhedral microcrystallites. Clusters of silver atoms did not separate within the polyhedra. On the boundaries, the particles of silver decorated and made visible a continuous three-dimensional network of linear dislocation segments meeting in triple nodes. Detailed studies could be made by focusing the microscope up and down through the network. This allowed the first observations within a crystal of the dislocation structure of (1) tilt subboundaries, (2) twist subboundaries, (3) subboundaries

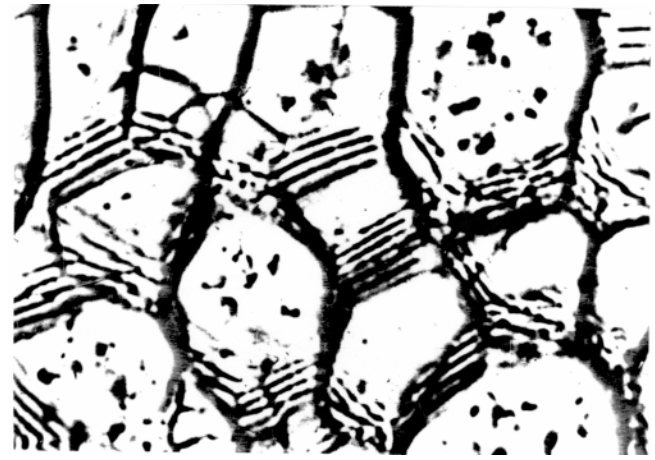


Figure 10. The mosaic structure of an AgBr crystal. Planar interfaces between polyhedral crystallites with tilt subboundaries having arrays of parallel edge dislocations and subboundaries with hexagonal networks of dislocations (X 3,330).²

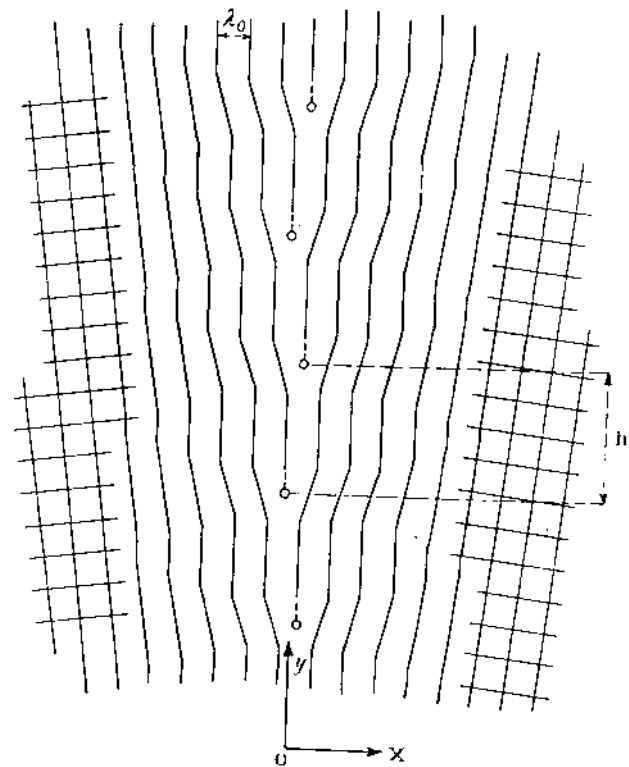


Figure 11. Model for a tilt subboundary between adjacent crystallites with a wall of equidistant parallel edge dislocations.²⁴

of arbitrary orientation, and (4) of planar triple nodes with three dislocations meeting in a point. The observations showed that the polyhedra of the mosaic structure had dimensions of the order of microns with misorientations between adjacent polyhedra of the order of minutes of arc as in the model of Darwin.

A model for a tilt subboundary between adjacent crystallites, formed by a wall of equidistant parallel edge dislocations, was proposed by Burgers in 1940 (Fig. 11) (Ref. 24). The tilt angle is given by $\theta = b/h$ where b is the magnitude of the Burgers vector and h the separation of the dislocations. The first photomicrograph of a tilt subboundary within a crystal is shown in Fig. 12. There is a wall of edge dislocations normal to the surface which appear as black spots where they intersect the focal surface of the



Figure 12. Small angle tilt boundary in fully annealed AgBr crystal having large subgrains with linear array of parallel edge dislocations normal to the surface (X 1,300).²

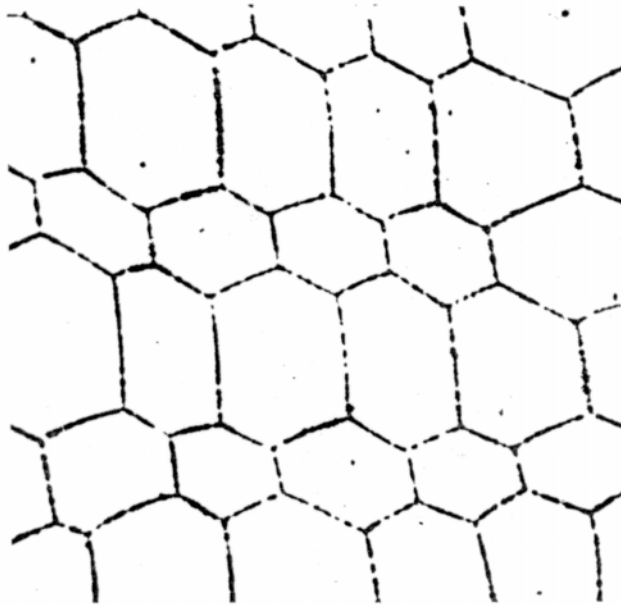


Figure 13. Small angle twist boundary in a fully annealed AgBr crystal formed by a hexagonal array of dislocation segments on a near {111} plane (X 3,590).²

microscope. The absence of particles of silver or of development centers within the remaining volume demonstrates the insensitivity of a dislocation-free volume of a crystal. The elastic strain energy is reduced by the formation of the boundary because regions of compression and tension for adjacent edge dislocations overlap and there are no long-range stresses. A twist subboundary is formed by a hexagonal array of screw dislocation segments on a {111} plane (Fig. 13). The size of the hexagonal elements decreases as the twist angle increases. These are examples of two particular orientations of mosaic boundaries in well-annealed crystals with very large subgrains. Between these are the orientations needed to produce the polyhedral mosaic structure of a crystal with its planar interfaces and continuous three-dimensional dislocation network of linear segments and triple nodes. These observations established the role of dislocations and substructures in the formation of internal latent-image, internal fog specks, and internal particles of

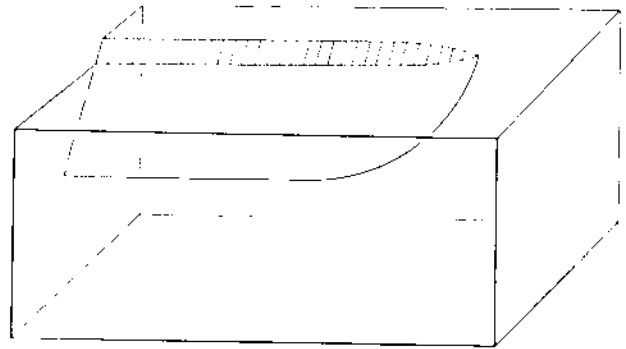


Figure 14. Elementary process for the initiation of plastic deformation. Creation of a surface terrace of unit width and a dislocation half-loop to relax the applied shear stress on an inclined glide plane.²

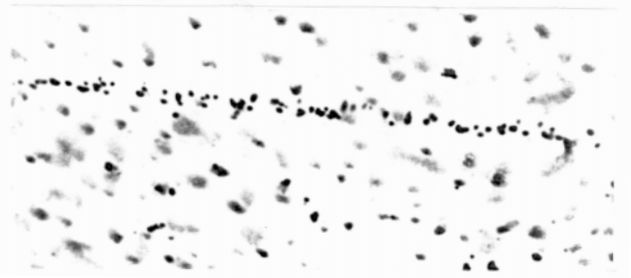


Figure 15. Terrace of Fig. 14, terminating at the dislocation line in the screw orientation, made visible by the preferential local formation of particles of surface photolytic silver (X 1,230).²

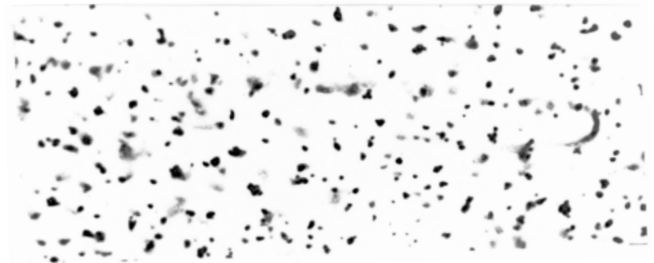


Figure 16. Photomicrograph 8 to 10 μm below the surface of Fig. 15 showing the decorated dislocation line in a jogged near screw orientation (X 1,230).²

photolytic silver. Silver did not separate within crystals without both lattice imperfections and donor centers.¹⁶⁻¹⁸

The plastic deformation of dislocation free crystals is initiated by the creation of dislocation half-loops on inclined glide planes at the surface by applied tensile or bending stresses (Fig. 14). These dislocations have edge and screw components and the half-loops are associated with a surface terrace. In crystals of AgCl and AgBr sensitized with Ag_2O and Ag_2 donor centers, both the terrace and the associated dislocation line below the surface are decorated by a minimum exposure with the separation of particles of silver.²⁵ The surface terrace terminating at the screw segment is shown in Fig. 15. The decorated jogged screw segment below the surface is seen in Fig. 16. The edge segment of the loop approximately parallel to the surface is shown in Fig. 17. The surface decoration rapidly disappears from solarization with continued exposure. This clearly establishes that surface terraces of unit width and dislocation lines have a role in photolytic processes in sensitized crystals. The observations illustrate the

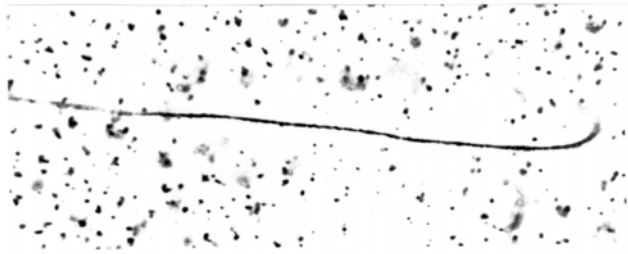


Figure 17. Photomicrograph 16 to 20 μm below the surface of Fig. 15 showing the decorated edge segment of the loop approximately parallel to the surface terrace (X 1,230).

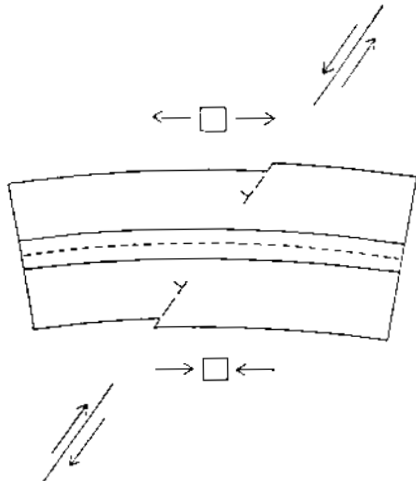


Figure 18. Creation of dislocation half-loops at (001) inclined surfaces of a tabular hexagonal microcrystal with two parallel twin planes subjected to bending stresses. The dotted line represents the neutral plane.³

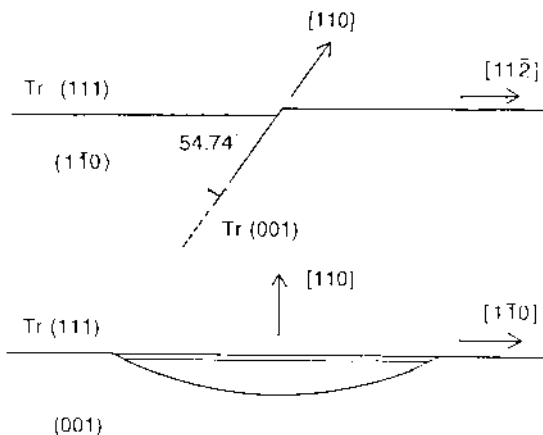


Figure 19. Creation of surface terrace of unit width and of dislocation half-loop on (001) plane at surface of tabular hexagonal crystal with (111) surfaces.³

elementary process of dislocation creation and displacement over a glide plane of Fig. 1.

Kink desensitization is a problem with silver halide emulsions coated on a flexible base. Tabular microcrystals are parallel to the substrate in the coatings. Dislocation half-loops in the edge orientation with a parallel surface terrace are generated by surface stresses created by sharp bending of the crystals on the substrate (Fig. 18). The resulting terrace and dislocation half-loop are shown in Fig. 19. Systems of such parallel surface-generated dislocation loops are seen in Fig. 20. The surface terraces are not decorated because of solarization.

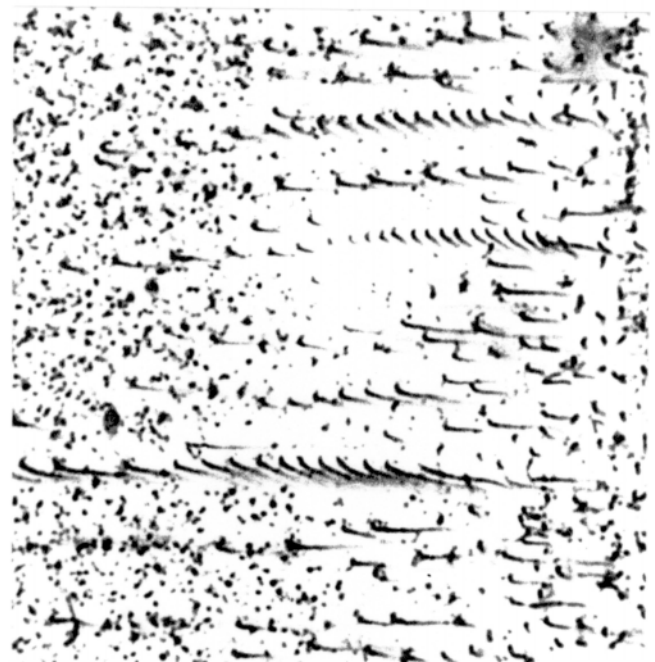


Figure 20. Systems of parallel decorated dislocation half-loops generated on approximately parallel glide planes at the surface of an AgBr crystal. The jogged segments meeting the surface in the near screw orientation are heavily decorated. The surface terraces are not decorated because of solarization (X 990). These loops were described as “intersecting the surface in the edge orientation” in the captions for Fig. 13 of Ref. 2. and Fig. 3 of reference 25. It has been established that these half-loops are of the type shown in Fig. 14 of this paper.

In the presence of internal chemical sensitization, internal Ag_n^+ latent-image clusters are formed along these dislocations during exposure. These clusters compete with the surface latent image for electrons giving rise to kink desensitization. Holes that cause surface solarization are also created by the decay of excitons at the internal Ag_n^+ centers during further exposure.¹ The Ag(Br,I) crystals, core/shell microcrystals, and microcrystals with a higher concentration surface iodide layer which require a higher shear stress for the creation and displacement of dislocations are less susceptible to kink desensitization than pure AgBr microcrystals.²⁶

Understanding of the internal separation of microscopically visible silver particles along dislocation lines still presented a problem in 1958. How could space for the separation of the particles with removal of the Cl⁻ or Br⁻ ions be made available in a crystal with Frenkel disorder and no mobile vacant halide ion lattice sites? The problem was resolved following experimental work in which glass spheres with a dimension of a few microns were incorporated in the crystals.²⁷ The shear stress field arising from differential contraction between the silver halide and the Pyrex glass on cooling from the melting point was relaxed by the formation at the interface of circular prismatic edge dislocation loops which glided away along one or more of the twelve radiating $\langle 110 \rangle$ directions (Fig. 21). This effectively resulted in the displacement of both X^- and Ag^+ ions away from the spheres.

The same systems of prismatic dislocation loops were then observed²⁸ on a smaller scale around particles of photolytic silver decorating circular prismatic dislocation loops in silver halide crystals with incorporated glass spheres sensitized with cuprous ions (Fig. 22). Six systems of prismatic dislocation loops radiating in a (111) plane along

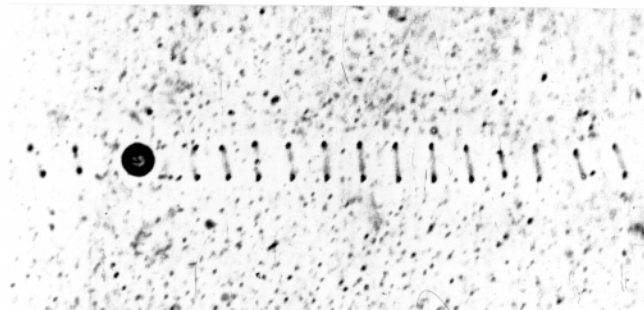


Figure 21. Sequence of circular prismatic edge dislocation loops along a $\langle 110 \rangle$ direction generated to relax the thermal stress field developed during cooling around a glass sphere embedded below the surface of an AgCl crystal near the temperature of the melting point (X 1,095).²

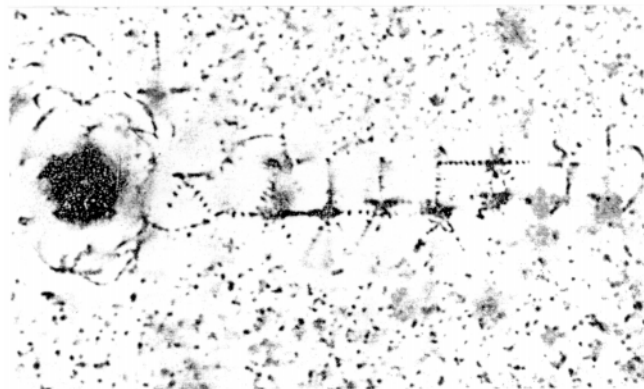


Figure 22. Sequence of circular prismatic edge dislocation loops generated in an AgCl (Cu⁺) crystal as in Fig. 21. The larger particles of decorating photolytic silver are themselves surrounded by systems of smaller prismatic loops along 12 radiating $\langle 110 \rangle$ directions (X 1,950).²⁸

$\langle \bar{1}10 \rangle$ directions from a growing particle of silver are shown in Fig. 23. Three more systems projected from the particle above this plane and three below, making twelve in all. The shear stress field responsible for the generation of the loops was created with chemical energy released by the aggregation of Ag atoms at small Ag_n⁺ nuclei. This provided a model for the growth of internal particles of photolytic silver.

Properties of Surface Sites of Termination of Dislocations

So far we have been concerned with the internal role of dislocations in silver halide crystals in photographic sensitivity. The sites of termination of dislocation segments at the surface of a crystal also have important functions. Visible particles of silver separate at these sites when crystals are exposed under a dilute solution of 1-phenyl-3-pyrazolidinone allowing nondestructive determination of the dislocation distribution and density.²⁹ Epitaxial nuclei of AgCl and Ag(Br,I) form at these sites on AgBr crystals.³⁰

The surface of a silver halide crystal in an aqueous medium is a dynamic interface with a high density of kinked surface terraces.³¹ These kink sites and terraces are involved in the dynamic processes of dissolution and crystal growth and adsorption and chemical reaction. The surface structure is stabilized and the rates of Ostwald ripening and chemical sensitization reduced by the adsorption of molecules of heterocyclic mercapto compounds at the kink sites and terraces. These rates are also decreased by the similar adsorption of iodide ions at the surfaces of AgBr crystals.

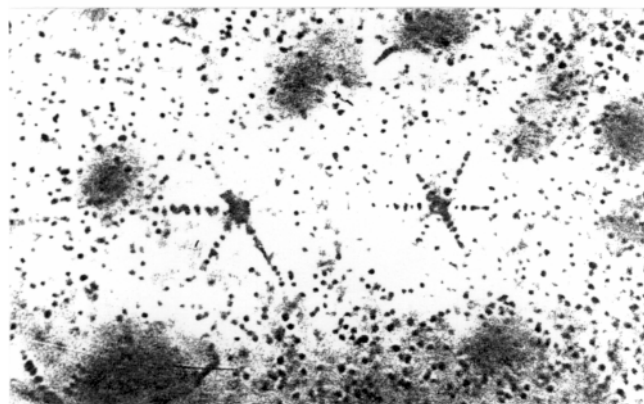


Figure 23. Systems of decorated prismatic edge dislocation loops radiating from particles of photolytic silver along six $\langle 110 \rangle$ directions in (111) planes in an AgCl(Cu⁺) crystal. Three more systems extended above and three below the plane along the remaining $\langle 110 \rangle$ directions (X 2,125).²

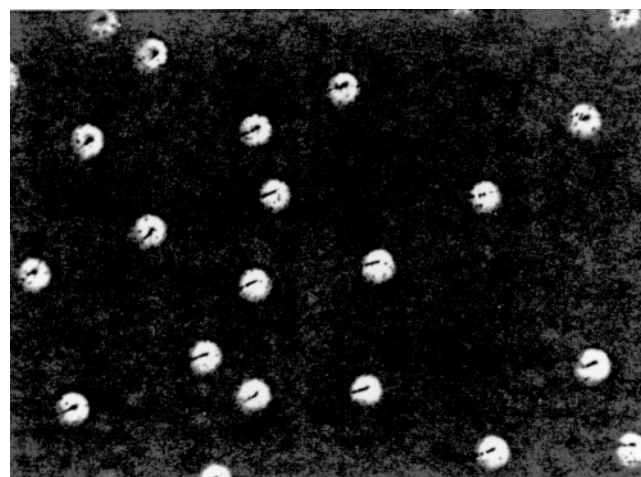


Figure 24. Phase-contrast photomicrograph showing depressions at points of termination of dislocations on the surface of an AgCl crystal produced by local dissolution in a solution of Na₂S₂O₃. Dislocations were subsequently made visible by decoration with photolytic silver (X 1,730).³²

There is an internal stress field around a dislocation that gives rise to a local increase in the elastic strain energy density. In the presence of particular solvents, the crystal passes into solution at the sites of termination of dislocations at a higher rate than over the remainder of the surface giving depressions with a high local density of reactive terraces and of kink sites along them. The depressions can be observed³² with a phase-contrast microscope and a one-to-one correspondence with sites of termination of dislocations established (Fig. 24).

In the dynamic competitive processes of dissolution, stabilization, and chemical sensitization, adsorbed molecules of stabilizers are more readily displaced by suitable solvent molecules and reactive chemical sensitizing molecules around the sites of termination of dislocations than over the remainder of the surface. The result is enhanced localized dissolution and preferential nucleation and growth of monolayer islands of (Ag,Au)S and Ag₂S molecules at these sites which are the sites of highest free energy density. Under the conditions of chemical sensitization, Ag₂O molecules are formed and adsorbed around the edges of the islands of sulfide molecules and reduced to adsorbed Ag₂ molecules. These provide latent-image growth nucleus precursors so that surface development centers are formed

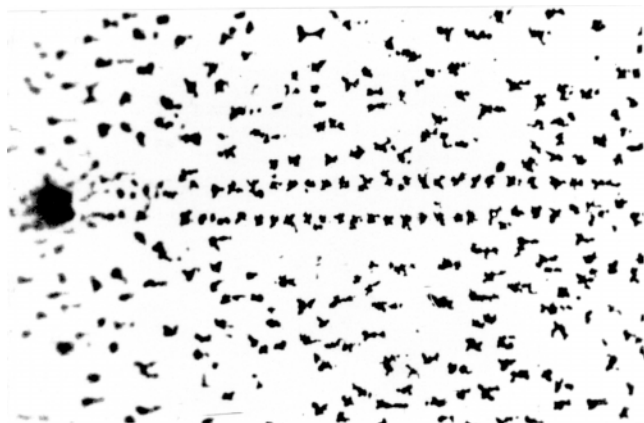


Figure 25. Development specks produced by interrupted development at sites of termination of prismatic edge dislocations in AgCl crystal immersed in a solution at pH 8 after treatment with a dilute $\text{Na}_2\text{S}_2\text{O}_3$ solution and then washed, dried, and exposed (X 1,500).²



Figure 26. Development centers formed at sites of termination of dislocations of the polyhedral subboundaries in a thin sheet AgCl crystal sensitized with a solution of $\text{Na}_2\text{S}_2\text{O}_3$ (X 1,725).⁶

preferentially at these sites. The initiation of chemical development which involves the localized passage of halide ions into solution is also favored at these sites because of the higher local free energy density.

The thin sheet crystals owe their effectiveness as a model system for the study of photographic sensitivity to their high density of dislocations and surface sites of termination of dislocations. Their properties were profoundly modified by annealing and recrystallization. The AgBr thin sheet crystals with near {001} surfaces were recrystallized with elimination of substructure and dislocations by slow passage through a steep temperature gradient. No image was produced when they were chemically sensitized, exposed, and developed with a surface developer. A dense image was formed by surface physical development, which showed efficient chemical sensitization.^{18,26} This experimental work established that the sites of termination of dislocations are needed for effective initiation of surface chemical development.

These and other properties were demonstrated by extensive experimental work carried out with thin sheet crystals of AgCl and AgBr. For the study of surface-terminating prismatic dislocation loops, crystals with glass spheres incorporated near the surface were used.^{26,32} The surface was dissolved to the level of the diametral planes of systems of

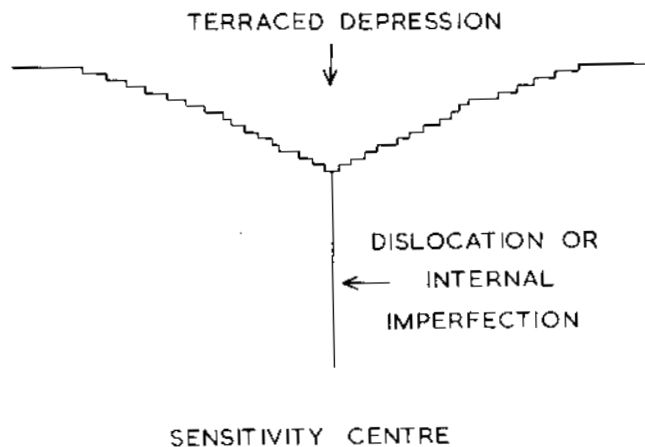


Figure 27. Model for a dislocation sensitivity center with a small terraced depression at the site of termination of a dislocation. The depression provides a site of enhanced reactivity for chemical sensitization and an internal latent image may be formed along the dislocation line.⁶

prismatic dislocation loops with a dilute solution of potassium cyanide that does not produce depressions at the termination sites of the dislocations. The surface was then treated with a dilute solution of sodium thiosulfate producing shallow local depressions at these sites. Treatment of the crystals with a buffer at pH 8 followed by washing, drying, exposure, and development gave development centers at the sites of termination of the prismatic dislocation loops (Fig. 25). This is important because these loops have the same nature as those that terminate around the edges of thin tabular structured grains. The same treatment of a thin sheet AgCl or AgBr crystal gave development centers at the sites of termination of dislocations of the subgrain boundaries (Fig. 26). These observations led to the introduction of the concept of the dislocation sensitivity center in 1958 (Fig. 27).⁶ Surface sites of termination of dislocations thus play an important role in the localization of products of chemical sensitization, in the concentration of Ag atoms during exposure, and in the initiation of chemical development.

Dislocations in Microcrystals of Silver Halides

The properties discussed so far were established mainly by experimental work with large thin sheet single crystals of pure AgCl and AgBr. We now have to consider the relevance of these observations to the microcrystals of commercial emulsions. The problem, is that the smallest observed separation of dislocations in AgCl and AgBr sheet crystals is about 1.5 μm . This is close to the maximum dimension of many emulsion microcrystals. If dislocations are to be relevant to the sensitivity of microcrystals, evidently conditions must exist in which higher density distributions can be produced.

We first consider the production of thin tabular dislocation free AgBr microcrystals. These provide the cores for AgBr core/Ag(Br,I) shell double-structure and triple-structure grains. Dislocations are high-energy lattice defects, the elastic strain energy of which increases the internal energy of a crystal by approximately 1.5 eV per plane of atoms traversed by the dislocation.¹³ In microcrystals, this energy is derived during growth from the excess chemical energy of the supersaturated system. Doubly twinned thin AgBr tabular nuclei with dislocations introduced at the high supersaturation nucleation stage are removed by preferential dissolution beginning at the dislocations during

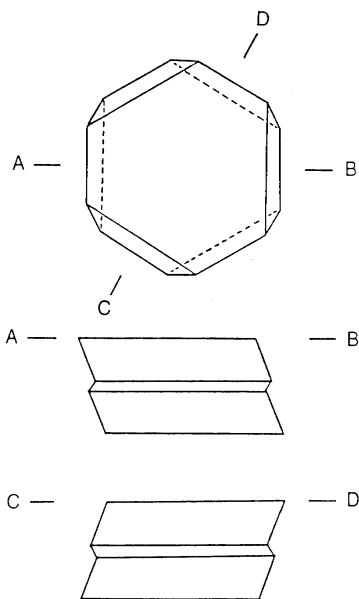


Figure 28. Tabular hexagonal AgBr microcrystal with two closely spaced parallel $\{111\}$ twin planes showing alternating acute and obtuse edges of major planes.³

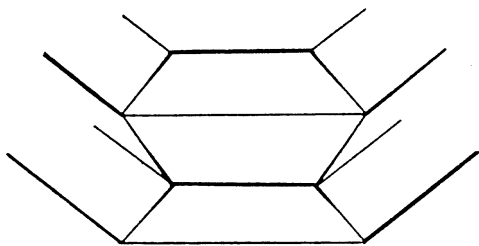


Figure 29. Structure of corners of lateral edges of tabular hexagonal microcrystal. Obtuse and acute edges at the major planes alternate around the crystal. These are associated with adjacent ridges and grooves at the twin planes. The intersections of the ridges and grooves define the corners of the twin planes. Nucleation of growth layers occurs at the grooves at these corners.

a brief period of ripening following nucleation.⁷ The remaining dislocation free hexagonal nuclei provide the most effective kinetic growth nuclei for further growth either by the balanced double-jet method or by the addition of a very fine dispersion of AgBr. An edge segment of the growth form of a doubly twinned microcrystal has an acute or obtuse edge at a $\{111\}$ plane with a groove or ridge at the adjacent twin plane. (Fig. 28). These are defined by the intersections of $\{11\bar{1}\}$ facets all parallel to the $\langle \bar{1}10 \rangle$ direction. Acute and obtuse edges having adjacent grooves and ridges at the twin planes alternate around the hexagonal crystal. The definition of these kinetic features may be lost by rounding of the edges at the conclusion of the growth process.

Nuclei for new edge growth layers with a central twin plane are formed at the corners at the reentrant grooves of the twin planes in the prevailing conditions of Br^- ion concentration and supersaturation (Fig. 29). Growth layers then spread away from these nuclei along the $\langle \bar{1}10 \rangle$ directions of the grooves and at a slower rate along the $\langle 01\bar{1} \rangle$ adjacent ridges of the twin planes. They also spread outward toward the major surfaces. Growth toward the major surfaces ceases when the $\{111\}$ elements of the leading edges of the growth layers reach the kinetic location

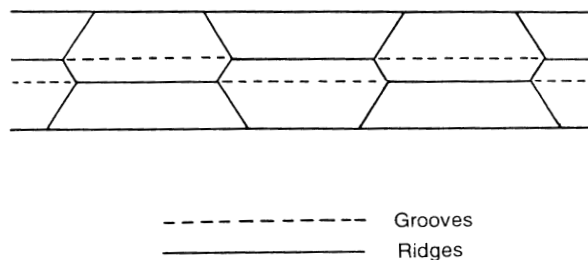


Figure 30. Net showing $\{11\bar{1}\}$ facets at three edges of a doubly twinned thin tabular hexagonal microcrystal. Sites defined by the intersection of grooves and ridges at the corners of the twin planes provide a symmetrical distribution of sites for nucleation of growth on $\{11\bar{1}\}$ facets.

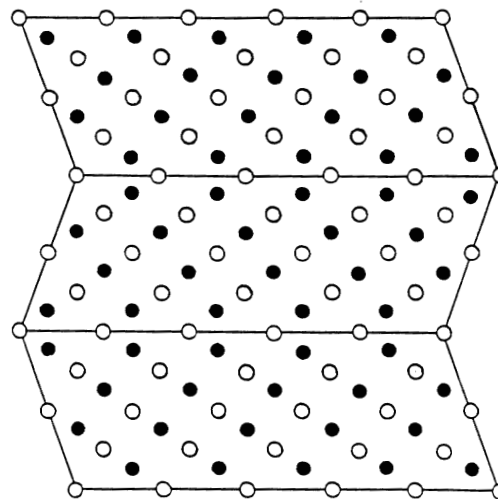


Figure 31. Atomic structure of $(\bar{1}10)$ plane in small volume of a silver halide crystal with two parallel twin planes showing the stacking sequence of $\{111\}$ planes. The boundary is defined by $\{111\}$ and $\{11\bar{1}\}$ planes that intersect the $(\bar{1}10)$ plane at right angles. Grooves at which nucleation occurs and ridges, both along $\langle \bar{1}10 \rangle$ directions, are represented.

of these surfaces (Fig. 30). On an atomic scale, the structure of the grooves and ridges along the twin planes is shown in Fig. 31. The grooves play a critical and essential role in the growth of twin planes of the tabular form in conditions where trigonal pyramidal and tetrahedral silver and halide ion complexes are involved,³³ particularly when iodide ions are incorporated in the complexes in Ag(Br,I) systems. The preferential outward radial growth at the edges of the microcrystals results in the production of a monodisperse distribution of thin hexagonal tabular AgBr microcrystals with plane major surfaces and a remarkably constant thickness. The microcrystals are free from dislocations and have a low level of internal sensitivity. The rates of nucleation and growth on the major surfaces are reduced, compared with the more rapidly growing edge facets, by the solute diffusion field and the slow adsorption of grain growth inhibitors. The Ag(Br,I) nucleation is shown at the corner groove sites of AgBr crystals in Fig. 32, a photomicrograph taken in 1954.³⁴

The most important method for the introduction of a stable controlled distribution and density of dislocations in tabular microcrystals depends on the establishment of steep local halide ion concentration gradients at the edges during growth.^{3,8,9} The elastic strain energy associated with a halide ion concentration gradient between two phases in a heterogeneous microcrystal is reduced by the nucleation of

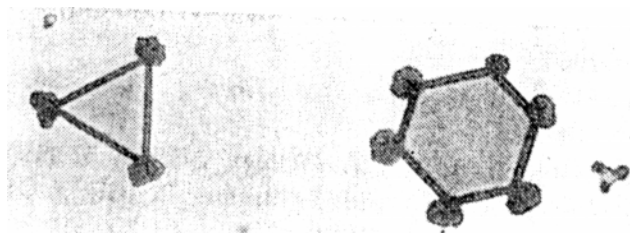


Figure 32. Formation of Ag(Br,I) nuclei at grooves at corners of triangular and hexagonal microcrystals of AgBr (X 2,960).³⁴

a statistical distribution of short segments of prismatic edge dislocation half-loops at the interfaces of the structured grains. These become elongated narrow prismatic edge dislocations with growth of succeeding shells.

For the statistically reproducible creation of dislocations, ultramicroscopic homogeneity of adjacent phases and lattice continuity across the interfaces are essential. Continuous grain growth without pauses which would allow adsorption of growth nucleation inhibitors and their incorporation by overgrowth is also essential. Unless these conditions are satisfied, the strain fields required for the regular nucleation of prismatic edge dislocation half-loops are not developed. The grains must also be all of the same composition with the same distribution of phases for individual grains.

In microcrystals, Ag(Br,I) phases of the necessary ultramicroscopic homogeneity within individual grains and statistical reproducibility between grains cannot be produced by the addition of a soluble iodide such as KI in controlled balanced double- or triple-jet methods. The iodide must be more uniformly distributed through the system before its incorporation in the grains. Two methods have been developed for the homogeneous incorporation of iodide ions in Ag(Br,I) elements. In the first, an ultrafine dispersion of Ag(Br,I) is produced in a high-speed external mixer and run into the reaction vessel with vigorous stirring and minimized intermediate Ostwald ripening.^{35,36} In the second, an iodide ion releasing compound such as 2-iodoethanol or sodium p-iodoacetamidobenzene sulfonate is distributed uniformly through the reaction vessel at pH 5 and temperature between 35°C and 60°C. The release of iodide ions is controlled by raising the pH to 9 to 10.5 and returning it to 5. (Refs. 37–39) The rapid and uniform release of iodide ions in the reaction vessel allows the steep iodide ion concentration gradients required for the introduction of statistically reproducible distributions of dislocations to be reliably produced. The supersaturation in the system increases as the diameter of the fine particles decreases and as the rate of release of iodide ions increases. A relatively high iodide ion concentration must be established for the introduction of higher density dislocation distributions.

There are three types of thin tabular structured grains with which controlled distributions of dislocations can be introduced.³ Double-structure grains have a dislocation free AgBr core and an Ag(Br,I) shell or a dislocation free Ag(Br,I) core with an AgBr or low iodide Ag(Br,I) shell. Triple-structure grains have a thin Ag(Br,I) annular zone within an AgBr core and an AgBr or low iodide Ag(Br,I) outer shell. The critical problem with dislocations in emulsion technology is to suppress internal latent image formation along dislocation lines while enhancing surface latent image formation at their sites of termination. Dislocations have to be introduced at internal and annular zone interfaces under mild oxidizing conditions to prevent the formation of associated Ag₂ latent image growth

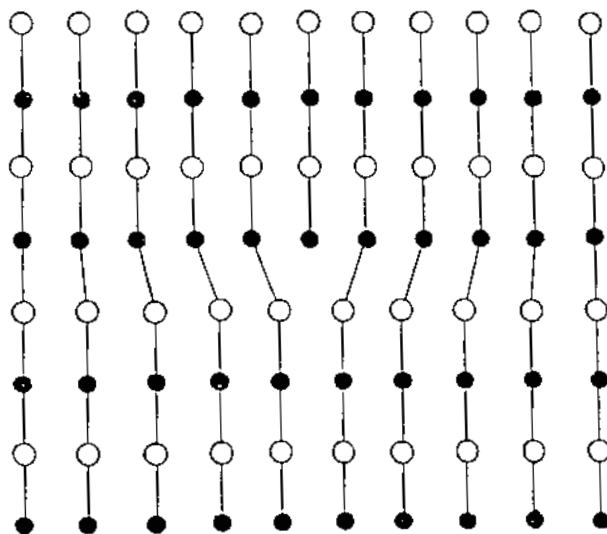


Figure 33. Atomic structure of $(11\bar{2})$ plane of an Ag(Br,I) core/AgBr shell microcrystal with an edge dislocation half-loop introduced at the phase interface to accommodate the mismatch of the lattice parameters.³

nucleus precursors.^{4,40} We will illustrate the general principles beginning with discussion of the Ag(Br,I) core/AgBr shell structure.

Doubly twinned ultramicroscopically homogeneous hexagonal Ag(Br,I) core grains, free from dislocations, stacking faults, and other lattice imperfections may be grown by Ostwald ripening of an ultrafine dispersion of Ag(Br,I) particles^{35,36} or by the use of an iodide ion releasing agent. They have a lattice parameter along the $\langle 110 \rangle$ directions of the edges which is larger than that of the subsequent AgBr growth layer and increases with the iodide concentration. Lattice mismatch occurs when the edge growth layers of an AgBr shell are nucleated at the grooves of the twin planes at the corners of the Ag(Br,I) cores and spread away rapidly along the grooves and ridges of the edges. Figure 33 shows the atomic structure in a $[\bar{1}10]$ direction along the groove at a twin plane. The increase in interfacial energy resulting from the lattice mismatch is reduced by the nucleation of a short segment of a prismatic edge dislocation half-loop across the groove of the twin plane to reduce the elastic strain. This dislocation has a Burgers vector, $\mathbf{b} = 1/2 a \langle 110 \rangle$ and results from the incorporation of rows of two additional half-planes of ions. The length of the segment is a fraction of the width of the edge. With further growth along the groove, a statistical distribution of approximately equidistant short half-loops may be successively nucleated as the mismatch at the leading edge of the growth layer along the $\langle 110 \rangle$ direction again reaches a lattice parameter. Outward growth on the oblique $\{11\bar{1}\}$ and $\{\bar{1}11\}$ facets ceases when the growth layers reach the kinetic location of the major $\{111\}$ planes resulting in the growth of tabular grains of uniform thickness with plane surfaces.

With an iodide concentration gradient across the interface, the linear density of prismatic edge dislocation half-loops is given by $\rho = 1.56\Delta[I]/\mu\text{m}$ where $\Delta[I]$ is the concentration difference across the growth plane in mole percent. This relation, first derived in 1957, applies across gradients arising from rapid changes in iodide concentration.^{8,9} For a linear projected density of 10 edge dislocations/ μm , $\Delta[I] = 6.4 \text{ mol}\%$. The maximum mean dislocation density introduced by a concentration gradient can be estimated by taking a Burgers circuit around the gradient. The closure failure of the corresponding circuit in a

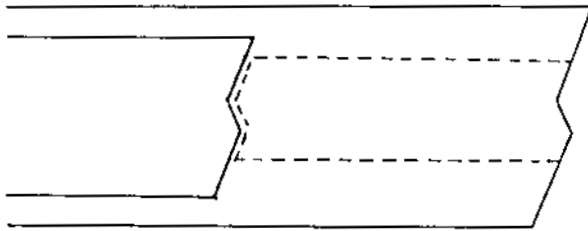


Figure 34. Narrow prismatic edge dislocation half-loop on $\{110\}$ plane of a doubly twinned Ag(Br,I) core/AgBr shell microcrystal. The loop was nucleated at the concentration gradient as a short segment across the groove at the twin plane and extended with continued growth along $\langle 112 \rangle$ directions through the shell to terminate at the edge and introduce two dislocation sensitivity centers.

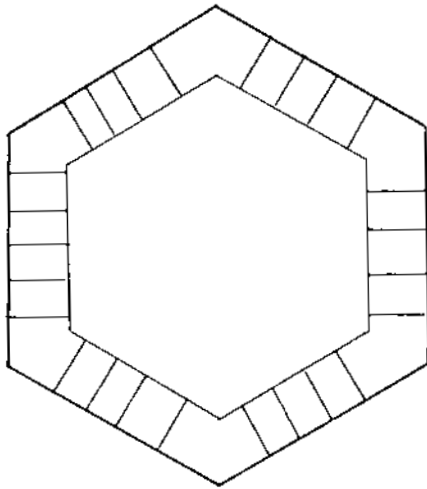


Figure 35. Narrow prismatic edge dislocation loops along $\langle 11\bar{2} \rangle$ directions, generated in the iodide ion concentration gradient at the Ag(Br,I) core/AgBr shell interface and terminating at the $\langle 110 \rangle$ edges of the grain.

homogeneous reference crystal divided by the Burgers vector and the area gives the mean density.

With continued growth of the microcrystal, the statistical distribution of short prismatic dislocation segments grows outward within the shell to give narrow prismatic dislocation half-loops with dislocations in a generally $\langle 11\bar{2} \rangle$ direction parallel to the major surfaces (Fig. 34). In optimum conditions, appearance of equidistant straight prismatic dislocations in this direction would be anticipated between the core/shell or annular zone interfaces and the edge of the crystal (Fig. 35). With relatively low density distributions, the dislocations can glide prismatically in the $\{111\}$ and $\{11\bar{1}\}$ planes to minimize their length and reduce their interaction energy. They terminate around the edges of the tabular grains to give dislocation sensitivity centers having the characteristics of those in Fig. 25 in which there are semicircular prismatic dislocation half-loops. This property would not be affected by rounding of the edges at the conclusion of growth.

What are probably prismatic dislocations are seen by diffraction contrast in the electron micrograph of an $\text{AgBr}_{0.9}\text{I}_{0.1}$ hexagonal microcrystal published by Ozeki, Urabe, and Tani⁴¹ in 1990. No details are given but it would appear that this is either a structured grain or dislocations arose from a fluctuation in iodide ion concentration. In agreement with the analysis already given, the Burgers vector of a similar dislocation was determined to be consistent with $\mathbf{b} = 1/2 a \langle 110 \rangle$ by Goessens and his coworkers in 1991.⁴²



μm

Figure 36. Transmission electron micrograph of a triple structure tabular emulsion grain showing dislocations between the annular zone phase interfaces and the edges of the grain.⁴³

The double-structure grain with an AgBr shell has advantages from the point of view of chemical sensitization and rapid initiation of chemical development. These advantages are shared by tabular triple-structure grains with an Ag(Br,I) annular zone for which no problems are experienced in producing dislocation free AgBr cores. Steep concentration gradients can be produced at the interfaces with the annular zone by the use of iodide ion releasing agents, and the dislocations introduced grow freely as narrow prismatic edge dislocation loops through the AgBr shell to terminate around the edge of the microcrystal. The prismatic dislocation loops and the associated halide ion concentration gradients are stable against both climb toward the $\{111\}$ major surfaces and thermal diffusion because of the immobility of the halide ions of the structure.

Figure 36 is a transmission electron micrograph of a triple-structure grain with an AgBr or low iodide Ag(Br,I) core and shell and a thin high iodide Ag(Br,I) annular zone.⁴³ Arrays of prismatic dislocation loops extend from the Ag(Br,I)/AgBr interfaces through the shell to terminate at the edges. They should have a Burgers vector, $\mathbf{b} = 1/2 a \langle 110 \rangle$ or $\langle 1\bar{1}0 \rangle$.

Triple-structure tabular grains also may have an AgBr core, a narrow internal annular zone having 6 to 10 mol% AgI and an outer shell with 2 to 3 mol% AgI. This has advantages for spectral sensitization and control of chemical development. With steep iodide concentration gradients at the two internal interfaces, 10 to 30 or more narrow prismatic edge dislocation loops may be nucleated and grown radially outward through the shell to terminate around the edges of the crystal. After chemical sensitization, these introduce dislocation sensitivity centers with adsorbed surface sulfide donor centers and Ag_2 latent-image growth nucleus precursors. It is evident that there will be a large number of equivalent sites for latent-image formation and that there must be an efficient concentration process if a development center is to be formed by the absorption of very few quanta. A possible mechanism is provided by the photoaggregation theory,^{1,4} according to which an Ag_4^+ or AuAg_3^+ latent-image growth nucleus is formed at an Ag_2 latent-image growth nucleus precursor following the absorption of one effective quantum. This releases from a donor center a photoelectron and either an Ag_0^+ or Au_0^+ interstitial ion which combines with an Ag_2 latent-image growth nucleus precursor to give an Ag_3 or AuAg_2 center. An Ag^+ ion is then adsorbed to give an Ag_4^+ or AuAg_3^+ latent-image growth nucleus. Although there may be many

sensitivity centers with Ag_2 molecules at terminating dislocations around the edges of the grain, one of these is distinguished from all the others as the site of formation of the first Ag_4^+ or AuAg_3^+ center. This photochemically produced latent-image growth nucleus or concentration center introduces a long-range Coulomb field. A second effective quantum then releases another photoelectron and Ag_0^+ or Au_0^+ ion from a donor center. In the Coulomb field, the electron is attracted to the positively charged Ag_4^+ or AuAg_3^+ center which provides a deep trap for it, and the positive charge is restored by the adsorption of an Ag^+ ion to give an Ag_5^+ or AuAg_4^+ development center. The two effective events create a positively charged development center of minimum size. One sensitivity center is thus selected, and the remaining centers are effectively desensitized giving an efficient concentration process for the growth of a limited number of development centers around the edges of the structured grains.⁴⁴⁻⁴⁷

Three essential elements are involved in the design and production of negative imaging, monodisperse, regular hexagonal, thin tabular silver halide microcrystals of the highest achievable performance. These are the introduction of statistically reproducible controlled distributions and densities of dislocations, donor centers, and latent-image growth nucleus precursors.

During this period of emphasis on applied research and product development, it is of interest to reflect that the search for understanding of the nature and distribution of the internal latent image, stimulated by Dr. Mees in 1949, led to the discovery of dislocations in 1952. This was followed by the establishment of dislocation properties and their important role in photographic sensitivity that has culminated in the production of the structured grains of recent commercial emulsions. ▲

Acknowledgment. The enthusiastic and effective collaboration of J. T. Bartlett, E. A. Braun, J. T. Burrow, P. V. McD. Clark, T. Evans, H. Hada, J. M. Hedges, D. A. Jones, H. D. Keith, and A. S. Parasnis in the experimental work on silver halide crystals is gratefully acknowledged.

References

- J. W. Mitchell, *J. Imaging Sci. Technol.* **39**: 193 (1995).
- J. W. Mitchell, *J. Soc. Photogr. Sci. Technol. Jpn.* **54**: 248 (1991).
- J. W. Mitchell, *J. Soc. Photogr. Sci. Technol. Jpn.* **54**: 258 (1991).
- J. W. Mitchell, *J. Photogr. Sci.* **42**: 2 (1994).
- J. W. Mitchell, *Proc. R. Soc. London, Ser. A* **371**: 149 (1980).
- J. W. Mitchell, *J. Photogr. Sci.* **6**: 57 (1958).
- M. Saitou, S. Urabe, and K. Ozeki, US Patent 4,797,354 (Jan. 10, 1989).
- J. W. Mitchell, Die photographische Empfindlichkeit, *Photogr. Korr.* **1**: Sonderheft (1957).
- J. W. Mitchell, *Photogr. Sci. Eng.* **27**: 81 (1983).
- F. C. Frank, *Phil. Mag.* **42**: 809 (1951).
- N. Thompson, *Proc. Phys. Soc. London Sect. B*, **66**: 481 (1953).
- J. Friedel, *Dislocations*, Addison-Wesley, Reading, MA, 1964.
- F. R. N. Nabarro, *Theory of Crystal Dislocations*, Clarendon Press, Oxford, 1967.
- J. P. Hirth and J. Lothe, *Theory of Dislocations*, 2nd Ed., John Wiley & Sons, New York, 1982.
- W. T. Read, *Dislocations in Crystals*, McGraw-Hill, New York, 1953.
- J. M. Hedges and J. W. Mitchell, *Philos. Mag.* **44**: 223 (1953).
- J. M. Hedges and J. W. Mitchell, *Philos. Mag.* **44**: 357 (1953).
- (a) T. Evans, J. M. Hedges and J. W. Mitchell, *J. Photogr. Sci.* **3**: 73 (1955); (b) T. Evans, *Crystal Imperfections and Chemical Reactivity*, Ph.D. Thesis, University of Bristol, 1955.
- C. G. Darwin, *Philos. Mag.* **27**: 315 (1914).
- C. G. Darwin, *Philos. Mag.* **27**: 675 (1914).
- C. G. Darwin, *Philos. Mag.* **43**: 800 (1922).
- W. L. Bragg, C. G. Darwin, and R. W. James, *Philos. Mag.* **1**: 897 (1926).
- R. W. James, *The Optical Principles of the Diffraction of X-Rays*, Bell, London, 1948.
- J. M. Burgers, *Proc. Phys. Soc. London* **52**: 23 (1940).
- J. T. Bartlett and J. W. Mitchell, *Philos. Mag.* **5**: 445 (1960).
- P. V. McD. Clark and J. W. Mitchell, *J. Photogr. Sci.* **4**: 1 (1956).
- D. A. Jones and J. W. Mitchell, *Philos. Mag.* **3**: 1 (1958).
- A. S. Parasnis and J. W. Mitchell, *Philos. Mag.* **4**: 171 (1959).
- J. W. Mitchell, in *Dislocations and Mechanical Properties of Crystals*, John Wiley & Sons, New York, 1957, p. 69.
- H. Hada and J. W. Mitchell, Technical Report AFAL-TR-153, Air Force Avionics Laboratory, Air Force Systems Command, Wright-Patterson Air Force Base, OH, 1972.
- J. W. Mitchell, *Photogr. Sci. Eng.* **26**: 270 (1982).
- D. A. Jones and J. W. Mitchell, *Philos. Mag.* **2**: 1047 (1957).
- E. Klein, *Photogr. Korr.* **92**: 139 (1956).
- J. W. Mitchell, *J. Soc. Photogr. Sci. Technol. Jpn.* **48**: 191 (1985).
- S. Urabe, US Patent 4,879,208 (Nov. 7, 1989).
- Y. Ichikawa, H. Ohnishi, S. Urabe, A. Kojima, and A. Katoh, US Patent 5,035,991 (July 30, 1991).
- Y. Suga, M. Kikuchi, M. Yagihara, H. Okamura, and H. Kawamoto, US Patent 5,418,124 (May 23, 1995).
- M. Kikuchi and H. Okamura, US Patent 5,498,516 (March 12, 1996).
- M. Kikuchi, M. Yagihara, H. Okamura, and H. Kawamoto, US Patent 5,527,664 (June 18, 1996).
- K. Ozeki, S. Urabe, and T. Tani, *J. Imaging Sci. Technol.* **34**: 136 (1990).
- C. Goessens, D. Schryvers, J. Van Landuyt, S. Amelinckx, A. Verbuck, and R. DeKeyser, *J. Crystal Growth* **110**: 930 (1991).
- H. Ikeda, M. Fujita, S. Ishimaru, H. Ayato, and S. Urabe, US Patent 4,806,461 (Feb. 21, 1989).
- J. W. Mitchell, *J. Imaging Sci. Technol.* **37**: 331 (1993).
- J. W. Mitchell, *Photogr. Sci. Eng.* **22**: 249 (1978).
- J. W. Mitchell, *J. Photogr. Sci.* **31**: 148 (1983).
- J. W. Mitchell, *J. Imaging Sci. Technol.* **31**: 1 (1987).
- J. W. Mitchell, *J. Imaging Sci. Technol.* **34**: 113 (1990).